



ROLE OF DIFFUSION WEIGHTED MR IMAGING IN EVALUATION OF INTRACRANIAL RING ENHANCING LESIONS

Radiology

Harshavardhana

Kuruba

Asst Professor, Department of Radiology, NIMS, Hyderabad, Telangana

Ramanjaneyulu

Chinmayee

Resident, Department of Radiology, NIMS, Hyderabad, Telangana *Corresponding Author

Biswal*

Jyotsna Rani

Professor, Department of Radiology, NIMS, Hyderabad, Telangana

Yarlagadda

Phani Chakravarty

Asst Professor, Department of Radiology, NIMS, Hyderabad, Telangana

Mutnuru

ABSTRACT

Aims and objectives: 1.To study the imaging findings and establish a differential diagnosis of various ring enhancing lesions on MRI.2.To differentiate neoplastic and non-neoplastic ring enhancing lesions using Diffusion Weighted Imaging.3.To differentiate primary and secondary neoplastic lesions using Diffusion Weighted Imaging.4.To correlate imaging findings of ring enhancing lesions with histopathological findings wherever possible.

Materials and methods: The study was done in Department of Radiology and Imageology, Nizam's Institute of Medical Sciences, Hyderabad from May 2014 to May 2016. 40 cases referred to the radiology department for MRI brain with clinical diagnosis / suspicion of focal cerebral ring enhancing lesions, irrespective of age and sex, were studied during this period. Both out-patients and in-patients were included in the study. Informed and written consent was taken from all the subjects participating in the study. The study was conducted using 1.5 Tesla MRI machine (Signa LX, GE).

Observations and results: In our study, 4 lesions showed diffusion restriction at the core (2 bacterial abscesses, 1 tuberculous abscess and 1 tuberculoma). All the other lesions (all but one tuberculomas, NCC granulomas, toxoplasma abscesses, primary glial neoplasms and metastasis) did not show diffusion restriction. We found significant difference in the ADC values at the core of tuberculomas and NCC granulomas ($p < 0.05$). The mean ADC values at the core of the restricted bacterial abscesses was $(67 \pm 3) \times 10^{-5} \text{ mm}^2/\text{s}$. The toxoplasma abscesses were evaluated with DWI showing absence of diffusion restriction and mean ADC values at the core as $(139.33 \pm 3) \times 10^{-5} \text{ mm}^2/\text{s}$. There was significant difference noted in the ADC values at the core of the brain abscess and neoplastic lesions, neoplastic and non neoplastic lesions ($p < 0.05$). There was also significant difference in the ADC values in the peritumoral region of the primary and secondary neoplastic lesions ($p < 0.05$). No significant difference was found in mean ADC values at the core of tuberculous and bacterial abscesses and between toxoplasma lesions and tuberculomas, primary and secondary neoplastic lesions.

Conclusions: DWI has a complimentary role in differentiating the neoplastic and non neoplastic lesions and in differentiating the etiology among the ring enhancing lesions.

KEYWORDS

Intracranial, Ring enhancing lesion, Diffusion Weighted Imaging(DWI), Apparent Diffusion Co-Efficient (ADC).

INTRODUCTION

Multiple intracranial ring-enhancing lesions are one of the most commonly encountered neuro imaging abnormalities. Widely available imaging techniques, computed tomography and magnetic resonance imaging (MRI) are used to detect these lesions.[1,3] A wide range of etiologies may present as cerebral multiple ring-enhancing lesions. On neuroimaging, these lesions appear as hypodense or isodense mass lesions on non-contrast computed (plain) tomography studies. After contrast administration, there is a ring- or a homogeneous disk-like enhancement within the region of hypodensity. The enhancing lesions are often of variable size and are usually surrounded by a varying amount of perifocal vasogenic edema. Typically, the ring-enhancing lesions are located at the junction of the gray and white matter, but they could be located in the sub-cortical area, deep in the brain parenchyma or may even be superficial.[2]

Diffusion weighted MRI (DW MRI) is a relatively recent MRI technique which provides image contrast that is different from that provided by conventional MR techniques. The uninhibited motion of water molecules is free diffusion. By contrast, the movement of water molecules in biologic tissues is restricted because their motion is modified and limited by interactions with cell membranes and macromolecules. The degree of restriction to water diffusion in biologic tissue is inversely correlated to the tissue cellularity and the integrity of cell membranes. Thus, DW MRI is based upon the principle of assessment of movement of water molecules (diffusion) in the pathological areas by applying magnetic gradients in various planes. Using DW MR sequences, the quantitative assessment of diffusion in the lesions can be obtained and is represented as Apparent

Diffusion Coefficient (ADC) values, which can be used for comparison between various pathologies.

BASICS OF DIFFUSION WEIGHTED IMAGING:

The basic principle of diffusion imaging is that the small random motion of the molecules results in a Gaussian distribution of phases. {4} The effect of these variations is enhanced by using a T2 weighted SE, gradient echo, or echo planar technique and applying strong gradients. The ability of these special pulse sequences to depict diffusion depends on the strength and duration of the diffusion gradients and on the direction in which they are applied. Diffusion is independent of the relaxation times and thus adds another factor to contrast. {5}

Apparent Diffusion Coefficient (ADC):

According to Fick's law, true diffusion is the net movement of molecules due to a concentration gradient. However, MR imaging, cannot differentiate molecular motion due to concentration gradients from molecular motion due to pressure gradients, thermal gradients or ionic interactions. Also, with MR imaging we do not correct for the volume fraction available or the increases in distance traveled due to tortuous pathways.

Therefore, when measuring molecular motion with DW imaging, only the apparent diffusion coefficient can be calculated. Substituting ADC for 'D', the signal intensity of a voxel on a DW image is thus expressed as

$$SI = SI_0 \times \exp(-b \times ADC)$$

AIMS AND OBJECTIVES : 1.To study the imaging findings and establish a differential diagnosis of various ring enhancing lesions on MRI. 2. To differentiate neoplastic and non-neoplastic ring enhancing lesions using Diffusion Weighted Imaging. 3.To differentiate primary and secondary neoplastic lesions using Diffusion Weighted Imaging. 4.To correlate imaging findings of ring enhancing lesions with histopathological findings wherever possible.

MATERIALS AND METHODS

- The study was done in Department of Radiology and Imageology, Nizam's Institute of Medical Sciences, Hyderabad.
- The study period was from May 2014 to May 2016.
- 40 cases referred to the radiology department for MRI brain with clinical diagnosis / suspicion of cerebral ring enhancing lesions, irrespective of age and sex, were studied during this period.
- Informed and written consent was taken from all the subjects participating in the study.

INCLUSION CRITERIA:

- All patients referred to MRI with clinically suspected neurological symptoms of infection / neoplasm.
- Cases of all age groups irrespective of sex will be included in the study.

EXCLUSION CRITERIA:

- Patients having general contraindications of MRI like history of claustrophobia and history of metallic implants insertion, cardiac pacemakers and metallic foreign body in situ.
- Unstable patients on life support mechanisms.

METHODOLOGY

The patients with clinical suspicion of ring enhancing lesion and referred from clinical departments for MRI brain study having ring enhancing lesions in the brain were included in the study. The study was done in Department of Radiology and Imageology, Nizam's Institute of Medical Sciences, Hyderabad from May 2014 to May 2016 after institute ethics committee approval.

Technique:

The study was conducted using 1.5 Tesla MRI machine (Signa LX, GE) Diffusion weighted MR sequence was performed at two 'b' values, $b = 0 \text{ s/mm}^2$ and $b = 1000 \text{ s/mm}^2$ to obtain axial index DW images. Then, by using a software application (FuncTool in GE Signa LX), Apparent Diffusion Coefficient (ADC) maps were obtained for each subject and for each lesion (if multiple lesions found in the same subject). The ADC values (measured in mm^2/s) at the core (center) of the lesion, periphery / enhancing rim of the lesion were recorded. In lesions that were too small or more linear on MR morphology or showed heterogeneous enhancement (not typically ring enhancing), in which ADC values could not be measured separately at the lesion core and the lesion periphery, the ADC values in the lesion were recorded at randomly selected more conspicuous areas in the lesion. A lesion was considered to be restricted if it was hyperintense to the normal white matter on DW index images and was hypointense on ADC maps with ADC value of less than $80 \times 10^{-5} \text{ mm}^2/\text{s}$ (48). Otherwise, the lesions were labelled as unrestricted on diffusion weighted imaging. NOTE – ADC values are usually expressed as $\times 10^{-3} \text{ mm}^2/\text{s}$. However for the

ease of calculations and statistical evaluation, in our entire study, the ADC values were expressed as $\times 10^{-5} \text{ mm}^2/\text{s}$.

The imaging parameters of the diffusion sequence were as follows-

TE: minimum 128,TR: 9000
 B- value: 1000 s/mm^2 , FOV: 240 mm
 Matrix size: 96×128 , Slice thickness: 5 mm
 Section spacing: 1.5 mm
 Planes – all, number of slices – 20.
 TR – time to repeat, TE – time to echo,
 TR and TE are in milli-seconds (ms)

Confirmation of the etiology of infection was considered according to the data obtained by cerebro-spinal fluid (CSF) analysis and other relevant laboratory investigations performed, clinical response to the treatment, in the form of symptomatic improvement / deterioration or looking for treatment response on follow up MRI scan in the form of reduced / increased perilesional edema or change in the number of lesions or lesion size.

Confirmation of primary brain neoplasms was done by surgical excision and histopathological diagnosis of the neoplasm.

Statistical Analysis –

Descriptive and analytical statistical analysis was carried out using the data obtained on Microsoft Excel software.

Continuous / quantitative data were stated as Mean \pm SD (Standard Deviation) and range while results on categorical / qualitative data were presented in numbers (%).

2-tailed Student independent t-test was used and P values calculated to assess the difference in the mean ADC values obtained in the study.

Significance was assessed at 5 % level of significance i.e. if P values were < 0.05 , the findings or the difference in the findings was considered significant. Various diagrams and charts were used to represent obtained data.

OBSERVATIONS AND RESULTS

The study population consists of 40 patients with intracranial ring enhancing lesions. The demographic profile of the study is as follows: Etiological distribution of patients:

Out of 40 patients, 28 patients had (70%) non neoplastic lesions and 12 had (30%) neoplastic lesions. Hence, in our study, non neoplastic ring enhancing lesions were more common than neoplastic lesions. Among the non neoplastic lesions, tuberculosis (64.2%) was the most common followed by NCC, toxoplasmosis and bacterial infection. Among the neoplastic lesions, metastasis (58.3%) was more common than primary neoplasm. So, the most common ring enhancing lesion encountered in our study was tuberculosis (40 %) with the least common being bacterial CNS infection (5 %). Total 5 patients were with HIV positive status; 1 of them had toxoplasmosis, infection, 3 had tuberculous infection and 1 patient had bacterial CNS infection in the form of abscess.

Table 1: The following table showing all the patients MR Diffusion & ADC findings.

Serial No	Age (years)	Sex	Diffusion restriction	ADC value in lesions [$\times 10^{-5} \text{ mm}^2/\text{s}$]			Peritumoral region	Final diagnosis
				Centre	Periphery / Wall	Normal white matter		
1	45	M	no	120	110	88		Tuberculomas
2	22	M	no	162	146	86		Neurocysticercosis
3	50	M	no	250	98	85	110	Glioblastoma multiforme
4	25	F	no	90.3	103	84.5		Tuberculous abscess
5	30	M	no	125,132	101,107	83,80		Tuberculoma
6	24	F	no	143,135	152,155	89, 79.5		Toxoplasma abscess
7	45	M	no	90	120	78		Tuberculoma
8	32	F	no	130	115	78		Tuberculomas
9	50	M	no	176	150	88		Neurocysticercosis
10	60	M	no	270	108	86	140	Metastasis
11	23	M	no	127, 138	103, 107.5	79.9,85		Tuberculomas
12	38	M	no	85,95	105,115	80,85		Tuberculomas
13	65	F	no	230	119	88	155	Metastasis
14	43	F	no	235	120	89	135	Anaplastic astrocytoma

15	33	F	no	135.5	107	81		Tuberculomas
16	35	F	no	155,160	145,150	70, 85		Neurocysticercosis
17	30	M	no	140	158	74.2		Toxoplasma abscess
18	55	M	no	256	120	78	132	Metastasis
19	66	F	no	240	105	80	120	Glioblastoma multiforme
20	25	F	no	86.5,81	112102.3	78,81		Tuberculomas with meningitis
21	13	F	no	125	103	80.3		Tuberculoma
22	52	M	no	235	113	80	150	Metastasis
23	18	F	no	150	130	85		Neurocysticercosis
24	23	F	yes	69,65	125,120	88,89		Bacterial abscess
25	65	M	no	230	100	85	122	Glioblastoma multiforme
26	40	F	no	250,200	110,115	81,79	170,153	Metastasis
27	25	M	no	134	113	74.5		Tuberculoma
28	54	M	no	165	140	78		Neurocysticercosis
29	31	F	no	130.5, 125	110.5, 110	81.5, 81		Tuberculomas
30	25	M	no	125.5	101	79		Tuberculomas
31	22	F	yes	70	110	76		Tuberculoma
32	52	M	no	220,265	106,100	77,88	160,138	Metastasis
33	42	M	no	250	110	79	138	Anaplastic astrocytoma
34	38	F	no	135	155	78.5		Toxoplasma abscess
35	50	F	no	240,230	123,125	79,80	166,150	Metastasis
36	30	F	no	79,83	108,110	78,76		Tuberculomas
37	55	M	no	160	137	90		Bacterial abscess
38	26	M	no	128	105	78.6		Tuberculoma
39	31	F	yes	72	110	86.5		Tuberculous abscess
40	24	F	no	126.8,139	102,103	86,83		Tuberculomas

Table 2. ADC values of the various ring enhancing lesions at core and periphery

Etiology	Core	Periphery
Tuberculomas T2 hypointense	129.42	106.5
Tuberculomas T2 hyperintense	84.75	110.32
NCC	161.6	142.2
Primary brain tumor	242	109.6
Metastasis	239.6	113.9
Toxoplasmosis	139.33	155
Bacterial abscess (with restriction)	67	122.5

Etiology wise ADC comparison-

The ADC values of the core of T2 hyper intense tuberculomas (84.75 +/- 4.9) x 10-5 mm2/s was significantly lower than that of NCC lesions (161 +/- 11.2) x 10-5 mm2/s with a p value of < 0.05.

The ADC values of the core of T2 hypo intense tuberculomas (129.42 +/- 4.5) x 10-5 mm2/s was significantly lower than that of NCC lesions (161 +/- 11.2) x 10-5 mm2/s with a p value of < 0.05.

The ADC values at the core of tuberculous abscesses (81.1 +/- 8.5) x 10-5 mm2/s and bacterial abscesses (67 +/- 3) x 10-5 mm2/s show no significant statistical difference (p>0.05).

The mean ADC values at the core of toxoplasmosis lesions [(139.33 +/- 3.7) x 10-5 mm2/s] do not show significant difference from that of tuberculomas [(129 +/- 5) x 10-5 mm2/s].

The ADC values of the core of bacterial abscess(67 +/- 3) x 10-5 mm2/s was significantly lower than that of primary neoplastic lesions (242 +/- 8.66) x 10-5 mm2/s.

The ADC values of the core of bacterial abscess(67 +/- 3) x 10-5 mm2/s was significantly lower than that of secondary neoplastic lesions (239.6 +/- 8.66) x 10-5 mm2/s.

The ADC values of the core of T2 hyper intense/ hypo intense tuberculomas (129 +/- 5) x 10-5 mm2/s was significantly lower than that of primary neoplastic lesions (242 +/- 8.66) x 10-5 mm2/s, secondary neoplastic lesions (239.6 +/- 8.66) x 10-5 mm2/s.

The ADC values of the core of NCC lesions (161 +/- 11.2) x 10-5 mm2/s was significantly lower than that of primary or secondary neoplastic lesions (242.5 +/- 8.66) x 10-5 mm2/s.

Comparison of ADC values of neoplastic and non- neoplastic lesions:

In our study, the ADC values at the core of non neoplastic lesions (123.7 +/- 5.4) x 10-5 mm2/s was significantly lower than that of neoplastic lesions (240.8 +/- 11.81) x 10-5 mm2/s with a p value of < 0.05. ROC curve analysis showed a cut off value of 188 x 10-5 mm2/sec at the core of the lesion with 100 % sensitivity and 99.92% specificity for distinguishing neoplastic and non neoplastic lesions with neoplastic lesions showing higher ADC values than the cut off value.

However, there was no significant difference in the ADC values at the periphery of the non neoplastic and neoplastic lesions.

Comparison of ADC values of primary and secondary ring enhancing lesions

When the ADC values of primary and secondary neoplastic lesions ring enhancing lesions were compared there was no significant difference in the ADC values at the core and the periphery between the both.

However, when the peritumoral region of the neoplastic lesions were compared, the metastatic lesions (151.4 +/- 10.55) x 10-5 mm2/s showed significantly higher ADC values in the peritumoral region than the primary glial neoplasms (125.5 +/- 9.88) x 10-5 mm2/s. ROC curve analysis showed a cut off value of 136.5 x 10-5 mm2/s at the peritumoral region with 90% sensitivity and 80% specificity for distinguishing primary and secondary lesions.

DISCUSSION

A total of 40 subjects (both outpatients and inpatients) referred to MRI with clinically suspected focal lesion in brain and those have already undergone conventional MRI sequences(plain and contrast) were subjected to diffusion weighted MR sequence on 1.5 Tesla MRI machine (Signa LX, GE) and results were analyzed.

The diffusion weighted MR findings and the ADC values in various etiologies of ring enhancing lesions were evaluated. The etiological confirmation of the diagnoses was considered according to the various laboratory investigations like blood and CSF analysis, radiological change in the number/ size of the lesions on follow up and histopathological confirmation, wherever required.

In our study, total 40 patients were studied with 20 males and 20 females. The mean age and age range was 37.1 years and 15 to 75 years.

A total of 80 focal lesions in 40 patients, (30 tuberculous, 20 NCC, 19 metastasis, 5 primary glial neoplasms, 3 bacterial and 3 toxoplasma)

were identified on the MRI sequences. The non neoplastic ring enhancing lesions(70%) were more common than neoplastic lesions(30%). Among the non neoplastic lesions, tuberculosis was the most common lesion (64%).

Out of 80 focal lesions, 75 lesions were seen on DW imaging with sensitivity of 93.75%. Out of which 50 lesions (24 tuberculous, 5 NCC, 10 metastasis, 5 primary glial neoplasm, 3 toxoplasma and 3 bacterial abscess) were adequately assessed by ADC maps. Rest of the lesions could not be adequately assessed because of the small size of the lesions and the inherent poor spatial resolution of the index DW images.

Tuberculosis (Figure 1)–

The mean ADC values at core of the T2 hypointense lesions, T2 hyperintense lesions and tuberculous abscesses were $(129.42 \pm 4.5) \times 10^{-5} \text{ mm}^2/\text{s}$, $(84.75 \pm 4.9) \times 10^{-5} \text{ mm}^2/\text{s}$ and $(81.1 \pm 8.5) \times 10^{-5} \text{ mm}^2/\text{s}$, respectively. There was no significant difference in the mean ADC values at the core of T2 hyperintense lesions and abscesses, while the core ADC of T2 hypointense lesions differed significantly from T2 hyperintense lesions and abscesses. Similar results were published in the study performed by Gupta RK et al {6},

The mean ADC at core of tubercular abscesses in our study was $(81.1 \pm 8.5) \times 10^{-5} \text{ mm}^2/\text{s}$. In study performed by Luthra G et al {7} the mean ADC value at the core was $(66 \pm 23) \times 10^{-5} \text{ mm}^2/\text{s}$. This difference in the values is due to the tubercular abscess without restriction having higher ADC value at the core and thus altering the mean. The ADC at the core of the abscess with restriction in our study was $73.3 \times 10^{-5} \text{ mm}^2/\text{s}$, which correlates well with the values in their study.

On comparing the ADC values at core, the ADC values at core of T2 hyper intense/ hypo intense tuberculomas $(129 \pm 5) \times 10^{-5} \text{ mm}^2/\text{s}$ was significantly lower than that of primary and secondary neoplastic lesions $(242 \pm 8.66) \times 10^{-5} \text{ mm}^2/\text{s}$, $239.6 \pm 10.2 \times 10^{-5} \text{ mm}^2/\text{s}$. ($p < 0.05$)

According to a study by S Chatterjee et al {8} observation there was overlap of mean ADC values of tuberculomas and metastasis. However, they had not compared the ADC values at the core of the lesions. But, in our study the ADC values at the core were compared and it was found that the ADC values at core of T2 hyper intense/ hypo intense tuberculomas $(129 \pm 5) \times 10^{-5} \text{ mm}^2/\text{s}$ was significantly lower than that of primary and secondary neoplastic lesions $(242 \pm 8.66) \times 10^{-5} \text{ mm}^2/\text{s}$.

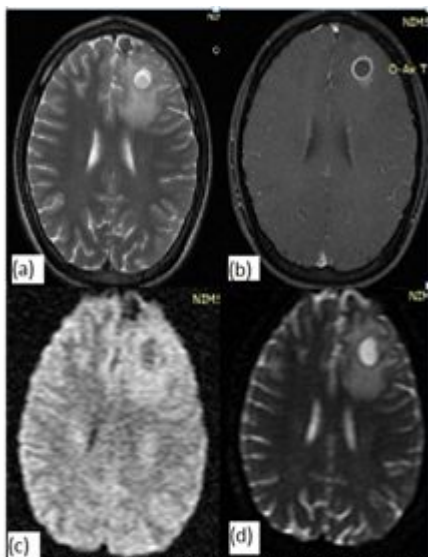


Figure 1: A 24 year old female with tuberculoma in left frontal lobe. Fig (a) shows heterogeneous lesion with mild perilesional edema on T2 weighted image; Fig (b) post contrast T1 image showing ring enhancing lesion; Fig (c) The lesion is hypointense on DW images suggestive of non-restriction, Fig (d) showing the ADC map. The ADC values at the core, periphery were $130 \times 10^{-5} \text{ mm}^2/\text{s}$, $115 \times 10^{-5} \text{ mm}^2/\text{s}$, respectively.

NCC–

In our study, the mean ADC at the core of NCC lesions was $(157.8 \pm 11.8) \times 10^{-5} \text{ mm}^2/\text{s}$ and was significantly higher ($p < 0.05$) than the ADC values at core of T2 hypointense as well as T2 hypointense tuberculomas. These findings correlate with a study done by Gupta RK et al [19] {6}, in which the mean ADC value from the core of the NCC lesions was $(166 \pm 29) \times 10^{-5} \text{ mm}^2/\text{s}$ and was significantly higher than the tuberculous granulomas.

Toxoplasmosis (Figure 2) :

In our study, three toxoplasmosis abscess were studied in two HIV positive male patients. Both abscesses showed peripheral enhancement and did not show restricted diffusion, with core and periphery / wall mean ADC values of $(139.33 \pm 3) \times 10^{-5} \text{ mm}^2/\text{s}$ and $(155 \pm 1.6) \times 10^{-5} \text{ mm}^2/\text{s}$.

Crispina H et al {9} studied diffusion-weighted MRI appearance of Toxoplasma abscesses. The findings correlate with those in our study in that there was absence of diffusion restriction in the toxoplasma abscesses.

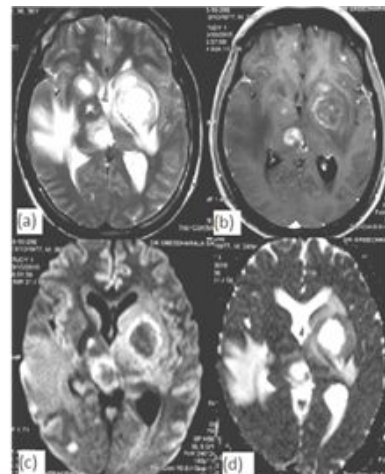


Figure 2: A 38 year old female with toxoplasmosis in RVD positive patient. Fig.(a) hyperintense lesions with perilesional edema in left basal ganglia and right thalamus on T2W image; Fig (b) post contrast T1W image shows peripherally enhancing abscess in left basal ganglia and nodular enhancing lesion in right thalamus, Fig. (c&d) shows non restriction of the abscess with core ADC value of $135 \times 10^{-5} \text{ mm}^2/\text{s}$ on DWI.

Bacterial Abscess (Figure 3):

In our study, 2 out of 3 (67%) bacterial abscesses showed restricted diffusion at the core with low mean ADC value of $(67 \pm 3) \times 10^{-5} \text{ mm}^2/\text{s}$ which correlates with the study done by Luthra G et al {10}, in which they obtained mean ADC of $(73 \pm 18) \times 10^{-5} \text{ mm}^2/\text{s}$ at the core of restricted bacterial abscesses. The core of bacterial abscess contains inflammatory cells, bacteria, mucoid proteins, cell debris along with necrosis and hence show restricted diffusion.

The abscess without restriction in our study was in a HIV positive patient with causative organism isolated as staphylococcus aureus. Non-restriction of the core in bacterial abscesses can occur as DWI findings differ based upon the variable concentrations of inflammatory cells and bacteria, different etiological organisms, the host immune response, a difference of the necrotic or viable inflammatory cells and the age of the abscess. In our study, the altered immune response of the HIV patient can probably be the explanation for the different diffusion characteristic (non-restriction) of the bacterial abscess.

There was significant difference in the mean ADC at the core of bacterial abscess $(67 \pm 3) \times 10^{-5} \text{ mm}^2/\text{s}$ and primary and secondary neoplastic lesions $(242 \pm 8.66) \times 10^{-5} \text{ mm}^2/\text{s}$, $239.6 \pm 10.2 \times 10^{-5} \text{ mm}^2/\text{s}$. ($p < 0.05$).

The findings were similar to the studies by Shigeo Ohba et al {11}, Noguchi et al {12}, Alam MS {13} et al, Ping Hong Lai et al {14} where significantly higher ADC values at the core of necrotic brain neoplasms were found when compared to lower ADC values at the core of brain abscess.

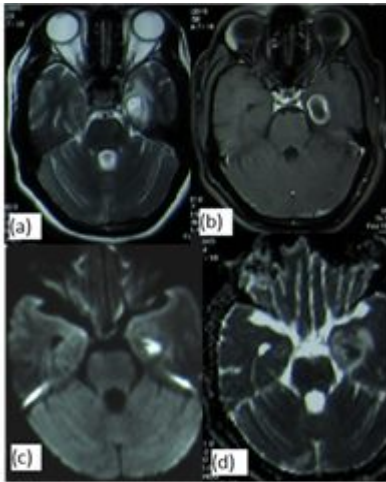


Figure 3: A 23 year old female with bacterial abscesses in left temporal lobe. Fig (a) T2 weighted image showing heterogeneously hyperintense lesion in left temporal lobe, Fig (b) post contrast T1 shows peripheral ring enhancement. The lesion is hyperintense on DW images with reversal on ADC map suggestive of restriction ;The ADC values at the core, periphery were $65 \times 10^{-5} \text{ mm}^2/\text{s}$, $120 \times 10^{-5} \text{ mm}^2/\text{s}$ respectively.

Primary Glial Neoplasms:

In our study, the mean ADC values at the core and the periphery of the primary glial neoplasm lesions was $(242 \pm 8.66) \times 10^{-5} \text{ mm}^2/\text{s}$ and $(109.6 \pm 7.5) \times 10^{-5} \text{ mm}^2/\text{s}$, respectively. These values correlate with the ADC values (mean \pm SD, $2.2 \pm 0.9) \times 10^{-3} \text{ mm}^2/\text{sec}$ in the cystic/necrotic portions, (mean \pm SD, $1.1 \pm 0.2) \times 10^{-3} \text{ mm}^2/\text{sec}$ in the peripheral enhancing portion of glioblastoma multiforme (Figure 4) in the study performed by Robert D. Tien et al {15}.

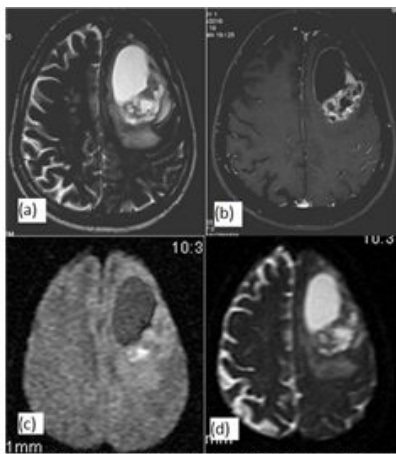


Figure 4: A 66 year old female with Glioblastoma multiforme in left frontal lobe. Fig (a) T2W image shows heterogeneous lesion with solid and cystic component in left frontal lobe. Fig (b) post contrast T1 image depicting irregular peripheral nodular enhancement. Fig (c) DWI images shows non restriction of the necrotic component and mild elevated signal of the solid component. Fig (d) shows corresponding ADC map. The ADC values at the core, periphery and peritumoral region in this case were $240 \times 10^{-5} \text{ mm}^2/\text{s}$, $105 \times 10^{-5} \text{ mm}^2/\text{s}$, $120 \times 10^{-5} \text{ mm}^2/\text{s}$ respectively.

The mean ADC values at the core of the primary glial neoplasms were significantly higher when compared to the ADC values at the core of the non neoplastic lesions.

Metastasis (Figure 5):

The mean ADC values of the lesions at the core and periphery / wall in our study were $(239.6 \pm 10.22) \times 10^{-5} \text{ mm}^2/\text{s}$ and $(113.9 \pm 7.8) \times 10^{-5} \text{ mm}^2/\text{s}$, respectively and were not significantly different from the ADC values of primary glial neoplasms.

The mean ADC values in the peritumoral region was $(151.4 \pm 9.8) \times$

$10^{-5} \text{ mm}^2/\text{s}$. The metastatic lesions show significantly higher ADC values than the primary glial neoplasms in the peritumoral region.

There was no significant difference in the mean ADC values at the core and the periphery of the primary glial neoplasms and the metastatic lesions. This correlated with the studies performed by Calli C et al {16}, Kathleen R. Fink et al {17}, Shigeo Ohba et al {18}, K Kono et al {19} where there was no difference noted in the ADC values of primary glial neoplasms ($230.9 \pm 74 \times 10^{-5}$), ($120.5 \pm 25 \times 10^{-5}$) and metastasis ($262 \pm 64 \times 10^{-5}$), ($129.3 \pm 41 \times 10^{-5}$).

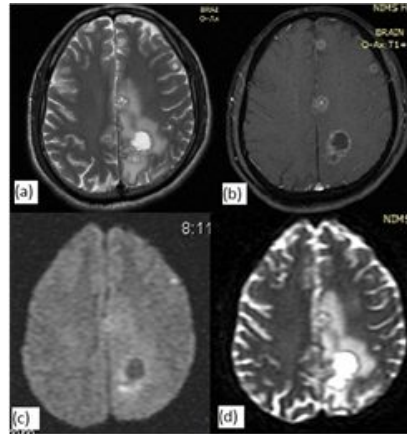


Figure 5: A 50 year old female with multiple cerebral metastasis from carcinoma of lung. Fig (a) Multiple heterogeneous lesions surrounded by disproportionate perilesional edema on T2 weighted image; Fig (b) Multiple irregular nodular ring enhancing lesions on post contrast T1; Fig (c) DWI depicting non restriction s/o facilitated diffusion in the centre with elevated signal in the periphery; Fig (d) shows ADC map. The ADC values at the core, periphery and peritumoral region in this case were $235 \times 10^{-5} \text{ mm}^2/\text{s}$, $113 \times 10^{-5} \text{ mm}^2/\text{s}$ and $150 \times 10^{-5} \text{ mm}^2/\text{s}$, respectively.

The mean ADC values in the peritumoral region of primary neoplasms was $(125.5 \pm 9.8) \times 10^{-5} \text{ mm}^2/\text{s}$. There was significant difference with p value <0.05 in the ADC values of the peritumoral region of primary glial neoplasms and the metastasis with metastasis showing higher ADC values than the primary glial neoplasms in the peritumoral region. This is due to the fact that in glioblastoma multiforme, the peritumoral region may be infiltrated with malignant cells in addition to vasogenic edema, whereas in a metastatic deposit, the peritumoral areas comprise predominantly vasogenic edema. Hence, there is restricted diffusion in the peritumoral region of glioblastoma when compared to the increased diffusion in metastasis.

A cut off of ADC value of $136.5 \pm 5.6 \times 10^{-5} \text{ mm}^2/\text{s}$ in the peritumoral region generated the best combination of 90% sensitivity and 80% specificity to differentiate the primary glial neoplasms and metastasis.

This correlated with the studies performed by Lee EJ et al {20}, Chiang IC et al {21} where a cutoff value of $1.302 \times 10^{-3} \text{ mm}^2/\text{s}$ for the minimum peritumoral ADC value generated the best combination of sensitivity and specificity for distinguishing between glioblastoma and metastasis with metastasis showing higher ADC values in the peritumoral region.

Comparison between ADC values of neoplastic and non neoplastic lesions at the core:

There is significant difference in the ADC values of non neoplastic lesions and neoplastic lesions. A cut off value of $188 \times 10^{-5} \text{ mm}^2/\text{s}$ at the core of the lesion generated the best combination of 100% sensitivity and 99.92% specificity for distinguishing neoplastic and non neoplastic lesions with neoplastic lesions showing higher ADC values than the cut off value. Hence, DWI has 100% sensitivity and 99.92% specificity for distinguishing neoplastic and non neoplastic lesions. The explanation for the higher ADC values is that the necrotic portion at the core of glioblastomas contain less viscous fluid with necrotic tumor tissue and few inflammatory cells thereby resulting in free diffusion of water molecules. In contrast the core of non-neoplastic inflammatory lesions contain inflammatory cells, bacteria, mucoid proteins, cell debris along with necrosis and hence show restricted diffusion.

According to earlier studies done by Shigeo Ohba et al {22}, Noguchi et al {23}, Alam MS {24} et al, Ping Hong Lai et al {25} showed that diffusion weighted imaging could be used to differentiate the brain abscess from necrotic brain neoplasms with significantly higher ADC values at the core of necrotic brain neoplasms when compared to lower ADC values at the core of brain abscess. These findings correlate with the findings in our study.

Comparison of diffusion characteristics in the wall / periphery of the lesions –

The mean ADC values in the wall / periphery of bacterial, tubercular, NCC and toxoplasmosis abscesses, primary glial neoplasms and metastasis were (122.5 +/- 2.5) x 10⁻⁵ mm²/s, (111.5 +/- 1.5) x 10⁻⁵ mm²/s, (142.2 +/- 2.5) x 10⁻⁵ mm²/s, (153.5 +/- 1.5) x 10⁻⁵ mm²/s, (109.6 +/- 7.5) x 10⁻⁵ mm²/s and (113.9 +/- 7.8) x 10⁻⁵ mm²/s respectively.

In study performed by Shigeo Ohba et al {26} the ADC_{mean} values of enhanced regions were 120 +/- 0.2x 10⁻⁵ mm²/s in glioblastomas, 129.3 +/- 0.4 x 10⁻⁵ mm²/s in metastasis and they were found not to differ significantly between metastatic tumors and glioblastomas. This finding correlated with the above ADC values in our study.

According to study done by Luthra G et al {27}, the mean ADC values in the wall of the pyogenic, tubercular abscesses were (79 +/- 19) x 10⁻⁵ mm²/s, (83 +/- 34) x 10⁻⁵ mm²/s respectively. As compared to this study, the values in our study are significantly higher. This probably was due to the difficulty in identifying correctly the wall of the lesions in many cases due to poor inherent spatial resolution of the DW index images and resultant placement of the region of interest (ROI) in the perilesional edema or adjacent brain parenchyma while calculating the ADC values in ADC maps.

According to our study there was no significant difference in the ADC values at the periphery between the non neoplastic and neoplastic lesions or the primary and secondary neoplastic lesions.

LIMITATIONS

- Limited number of subjects in the study. More number of subjects could have made the statistical analysis more accurate.
- All lesions were not histo pathologically proven.
- Small lesions could not be evaluated by diffusion and ADC maps

CONCLUSION

- DWI has a complimentary role in differentiating the neoplastic and non neoplastic lesions and in differentiating the etiology among the ring enhancing lesions.

ABBREVIATIONS

ADC – Apparent diffusion coefficient
 AIDS – Acquired immunodeficiency syndrome
 CNS – Central nervous system
 CSF – Cerebrospinal fluid
 CT – Computed tomography
 DW – Diffusion weighted
 DWI – Diffusion weighted imaging
 EP – Echoplanar
 EPI – Echoplanar imaging
 FLAIR – Fluid attenuated inversion recovery
 FSE – Fast spin echo
 HIV – Human immunodeficiency virus
 Max – Maximum
 Min – Minimum
 mm – Millimeters
 MR – Magnetic resonance
 MRA – Magnetic resonance angiography
 MRI – Magnetic resonance imaging
 ms – Milliseconds
 NCC – Neurocysticercosis
 NMR – Nuclear magnetic resonance
 s – Seconds
 SD – Standard deviation
 sec – Seconds
 T1W – T1 weighted
 T2W – T2 weighted
 TB – Tuberculosis
 TBM – Tuberculous meningitis
 TE – Time to echo

TR – Time to repeat
 WBC – White blood cells

REFERENCES

- {1} Cunliffe CH, Fischer I, Monoky D, Law M, Revercomb C, Elrich S, et al. Intracranial lesions mimicking neoplasms. Arch Pathol Lab Med 2009; 133; 101-23.
- {2} Patterns of contrast enhancement in brain and meninges. Radiographics, 2007; 27, 525-5.
- {3} Omuro AM, Leite CC, Mokhtari K, Delattre JY. Pitfalls in the diagnosis of brain tumours. Lancet Neurol 2006; 5, 937-948.
- {4} Allen PS. Some fundamental principles of Nuclear magnetic resonance in medical physics, Monograph No.21: The physics of MRI. New York: AIP press; 1992.p.15-21
- {5} Abragam A. The principles of nuclear magnetism. London: Oxford University Press; 1961.
- {6} Gupta RK, Prakash M, Mishra AM, Husain M, Prasad KN, Husain N. Role of diffusion weighted imaging in differentiation of intracranial tuberculoma and tuberculous abscess from cysticercus granulomas-a report of more than 100 lesions. Eur. J. Radiol. Elsevier; 2005;55(3):384-92.
- {7} Luthra G, Parihar A, Nath K, Jaiswal S, Prasad KN, Husain N, et al. Comparative evaluation of fungal, tubercular, and pyogenic brain abscesses with conventional and diffusion MR imaging and proton MR spectroscopy. Am. J. Neuroradiol. Am Soc Neuroradiology; 2007;28(7):1332-8.
- {8} S. Chatterjee, J.Saini,C.Kesavadas, differentiation of tubercular infection and metastasis presenting as ring enhancing lesion by diffusion and perfusion magnetic resonance imaging. Journal of Neuroradiology, 2010, 37, 167-171.
- {9} Crispina H, Chong-Han CH, Cortez SC, Tung GA. Diffusion-weighted MRI of cerebral toxoplasma abscess. Am. J. Roentgenol. Am Roentgen Ray Soc; 2003;181(6):1711-4.
- {10} Luthra G, Parihar A, Nath K, Jaiswal S, Prasad KN, Husain N, et al. Comparative evaluation of fungal, tubercular, and pyogenic brain abscesses with conventional and diffusion MR imaging and proton MR spectroscopy. Am. J. Neuroradiol. Am Soc Neuroradiology; 2007;28(7):1332-8.
- {11} Shigeo Ohba, Takakazu Ushioda, Toru Nakagawa, Kazuhiko Shimizu, Hideki Murakami, Diffusion magnetic resonance imaging for enhanced visualization of malignant cerebral tumors and abscesses, Neurology India, Vol. 59, No. 5, September-October, 2011, pp. 674-678.
- {12} Noguchi K, Watanabe N, Nagayoshi T, Kanazawa T, Toyoshima S, Shimizu M, et al. Role of diffusion-weighted echo-planar MRI in distinguishing between brain abscess and tumour: a preliminary report. Neuroradiology, Springer; 1999;41(3):171-4.
- {13} Alam MS1, Sajjad Z, Azeemuddin M, Khan ZA, Mubarak F, Akhtar W, Diffusion weighted MR imaging of ring enhancing brain lesions, J Coll Physicians, SurgPak. 2012 Jul;22(7):428-31. doi: 07.2012/JCPSP.428431
- {14} Ping-Hong Lai, Shu-Shong Hsu, Yuk-Keung Lo, and Shang-Wu Ding, Role of Diffusion-Weighted Imaging and Proton MR Spectroscopy in Distinguishing between Pyogenic Brain Abscess and Necrotic Brain Tumor AJNR 2002 23: 1369-1377.
- {15} Robert D. Tieni ,Gary J. Felsberg, Henry Friedman, Mark Brown, James MacFalli, MR Imaging of High-Grade Cerebral Gliomas: Value of DiffusionWeighted Echoplanar Pulse Sequences, AJR:162, March 1994
- {16} Cem Calli, Omer Kitis, Nilgun Yuntun, Perfusion and diffusion MR imaging in enhancing malignant cerebral tumors, European Journal of Radiology, Volume 58, Issue 3, June 2006, Pages 394-403
- {17} Kathleen R. Fink* and James R. Fink, Imaging of brain metastases, Surg Neurol Int. 2013; 4(Suppl 4):S209-S219.
- {18} Shigeo Ohba, Takakazu Ushioda, Toru Nakagawa, Kazuhiko Shimizu, Hideki Murakami, Diffusion magnetic resonance imaging for enhanced visualization of malignant cerebral tumors and abscesses, Neurology India, Vol. 59, No. 5, September-October, 2011, pp. 674-678.
- {19} Kono K, Inoue Y, Nakayama K, Shakudo M, Morino M, Ohata K, et al. The role of diffusion-weighted imaging in patients with brain tumors. AJNR Am J Neuroradiol 2001;22:1081-8.
- {20} Lee EJ, terBrugge K, Mikulis D, Choi DS, Bae JM, Lee SK, et al. Diagnostic value of peritumoral minimum apparent diffusion coefficient for differentiation of glioblastoma multiforme from solitary metastatic lesions. AJR Am J Roentgenol. 2011;196:71-6.
- {21} Chiang IC Kuo YT, Lu CY, Yeung KW, Lin WC, Sheu FO, Liu GC, Distinction between high-grade gliomas and solitary metastases using peritumoral 3-T magnetic resonance spectroscopy, diffusion, and perfusion imagings, Neuroradiology 46(8):619-27 · September 2004.
- {22} Shigeo Ohba, Takakazu Ushioda, Toru Nakagawa, Kazuhiko Shimizu, Hideki Murakami, Diffusion magnetic resonance imaging for enhanced visualization of malignant cerebral tumors and abscesses, Neurology India, Vol. 59, No. 5, September-October, 2011, pp. 674-678
- {23} Castillo M. Imaging brain abscesses with diffusion-weighted and other sequences. Am. J. Neuroradiol. American Society of Neuroradiology; 1999;20(7):1193-4.
- {24} Alam MS1, Sajjad Z, Azeemuddin M, Khan ZA, Mubarak F, Akhtar W, Diffusion weighted MR imaging of ring enhancing brain lesions, J Coll Physicians, SurgPak. 2012 Jul;22(7):428-31. doi: 07.2012/JCPSP.428431.
- {25} Ping-Hong Lai, Shu-Shong Hsu, Yuk-Keung Lo, and Shang-Wu Ding, Role of Diffusion-Weighted Imaging and Proton MR Spectroscopy in Distinguishing between Pyogenic Brain Abscess and Necrotic Brain Tumor AJNR 2002 23: 1369-1377.
- {26} Shigeo Ohba, Takakazu Ushioda, Toru Nakagawa, Kazuhiko Shimizu, Hideki Murakami, Diffusion magnetic resonance imaging for enhanced visualization of malignant cerebral tumors and abscesses, Neurology India, Vol. 59, No. 5, September-October, 2011, pp. 674-678.
- {27} Luthra G, Parihar A, Nath K, Jaiswal S, Prasad KN, Husain N, et al. Comparative evaluation of fungal, tubercular, and pyogenic brain abscesses with conventional and diffusion MR imaging and proton MR spectroscopy. Am. J. Neuroradiol. Am Soc Neuroradiology; 2007;28(7):1332-8.